

## Non-Fickian tracer transport in porous media

José A. Ferreira<sup>1</sup> and Luís Pinto<sup>1</sup>

<sup>1</sup> *CMUC, Department of Mathematics, University of Coimbra, Portugal*

emails: [ferreira@mat.uc.pt](mailto:ferreira@mat.uc.pt), [luisp@mat.uc.pt](mailto:luisp@mat.uc.pt)

### Abstract

Diffusion processes have traditionally been modeled using the classical diffusion equation. However, as in the case of tracer transport in porous media, significant discrepancies between experimental results and numerical simulations have been reported in the literature. Therefore, in order to describe such anomalous behavior known as non-Fickian diffusion, some authors have replaced the parabolic model by continuous random walk models, which have been shown to be very effective. Integro-differential models have been also proposed to describe non-Fickian diffusion in porous media. The aim of this paper is to compare the ability of these classes of models to capture the dynamics of tracer transport in porous media.

*Key words: tracer transport, porous media, non Fickian diffusion, CTRW, numerical simulation.*

## 1 Introduction

Trance transport in porous media is generally described by a diffusion equation that depends on the fluid velocity, which is linked to the pressure by the Darcy's law (see [24], [9], [12], [23] and [28]). Such diffusion equation is established considering the mass conservation equation

$$\frac{\partial u}{\partial t} + \nabla \cdot (vu) = \nabla \cdot J + q_2, \quad (1)$$

where  $u$  denotes the concentration,  $v$  the fluid velocity,  $J$  the mass flux and  $q_2$  a reaction term. In (1)  $J$  is given by

$$J = J_{dif} + J_{dis}, \quad (2)$$

where  $J_{dif}$  denotes the mass flux due to molecular diffusion

$$J_{dif} = -D_m \nabla u, \quad (3)$$

where  $D_m$  is the effective molecular diffusion tensor, and  $J_{dis}$  satisfies the so called Fick's law  $J_{dis} = -D_d \nabla u$ , and represents the dispersive mass flux associated with random deviations of fluid velocities within the porous space from their macroscopic value  $v$ . In the definition of  $J_{dis}$ ,  $D_d$  denotes the dispersive tensor usually given by  $D_d = \alpha_t \|v\| I + (\alpha_\ell - \alpha_t) \frac{1}{\|v\|} v v^T$ , where  $\alpha_\ell$  and  $\alpha_t$  are the longitudinal and transversal dispersivities.

Combining (1) with (2) we obtain the parabolic equation

$$\frac{\partial u}{\partial t} + \nabla \cdot (uv) = \nabla \cdot ((D_m I + D_d) \nabla u) + q_2, \quad (4)$$

where  $I$  is the identity tensor. Equation (4) can be rewritten in the following equivalent form

$$\frac{\partial u}{\partial t} + \nabla \cdot (uv) = \nabla \cdot (D \nabla u) + q_2. \quad (5)$$

The use of equation (5) to describe diffusion processes in porous media in general and tracer transport in particular have been shown inefficient. In fact the numerical results obtained do not accurately reproduce the laboratorial experiments. These facts are well reported in the literature and without be exhaustive we mention [2], [5], [6], [16], [18], [19], [20], [26], [27] and [30]. Several limitations of the parabolic equation to describe the concentration evolution have been pointed out (see, for instance, [4], [17], [21]): it prescribes an infinite speed of propagation for the concentration; it is based on Fick's law for the mass flux which establishes a linear relation between the concentration and dispersive mass flux; the mass flux  $J$  is independent of the history of dispersion; in the dispersive tensor the dispersive coefficients are medium constant and invariant with time and space (often they increase with the distance and/or with time). To circumvent the pathological behavior of the diffusion equation (5) several approaches were proposed in the literature. A summary of some of them is given in [21].

A widely adopted alternative is based on continuous time random walks (CTRW) (see for instance [2], [5], [6], [8], [15], [18], [19]). Let us consider that each particle in diffusion performs jumps or transitions characterized by waiting times between jumps. The jumps and the waiting time are coupled by a joint probability density function (pdf)  $\psi$  that describes at  $(x, t)$  the jump at position  $x$  and time  $t$ . When the jumps occur in  $\mathbb{R}^n$ , the pdf  $\psi$  and  $u$  are linked by the following generalized master equations

$$\frac{\partial u}{\partial t}(x, t) = \int_0^t \frac{1}{t_1} \left( \int_{\mathbb{R}^n} M(x-z, t-\sigma) u(z, \sigma) dz - \int_{\mathbb{R}^n} M(z-x, t-\sigma) u(x, \sigma) dz \right) d\sigma. \quad (6)$$

In (6)  $t_1$  represents a median transition time,  $M(x, t)$  is defined by its Laplace transform  $\tilde{M}(x, s)$  which is given by

$$\tilde{M}(x, s) = \frac{st_1 \tilde{\psi}(x, s)}{1 - \tilde{\psi}(u)}. \quad (7)$$

In (7) the following notations were used:  $\tilde{\psi}(x, s)$  represents the Laplace transform of the pdf  $\psi(x, t)$  and  $\tilde{\psi}(s) = \int_{\mathbb{R}^n} \tilde{\psi}(x, s) dx$ . If we assume that the pdf  $\psi$  is such that its Laplace transform can be decoupled in the following form  $\tilde{\psi}(x, s) = p(x)\tilde{\phi}(s)$  where  $p(x)$  denotes the transition length pdf and  $\phi$  denotes the marginal density of  $\psi$ , then  $\tilde{M}$  admits also the decoupling  $\tilde{M}(x, s) = p(x)\tilde{M}(s)$ , where

$$\tilde{M}(s) = \frac{st_1\tilde{\phi}(s)}{1 - \tilde{\phi}(s)}.$$

From (6), we have in the Laplace space the following generalized mater equation

$$s\tilde{u}(x, s) - u_0(x) = \frac{1}{t_1}\tilde{M}(s)\left(\int_{\mathbb{R}^n} p(x-z)\tilde{u}(z, s)dz - \int_{\mathbb{R}^n} p(z-x)\tilde{u}(x, s)dz\right),$$

which is equivalent to

$$s\tilde{u}(x, s) - u_0(x) = \frac{1}{t_1}\tilde{M}(s) \sum_{|\alpha|} (-1)^{|\alpha|} \frac{1}{\alpha!} m_{\alpha,p} \frac{\partial^{|\alpha|}\tilde{u}}{\partial x^\alpha}(x, s), \quad (8)$$

where  $\alpha = (\alpha_1, \dots, \alpha_n)$ ,  $\alpha_i \in \mathbb{N}_0$ ,  $|\alpha| = \sum_{i=1}^n \alpha_i$ ,  $\alpha! = \prod_{i=1}^n \alpha_i!$ ,  $\frac{\partial^{|\alpha|}\tilde{u}}{\partial x^\alpha} = \frac{\partial^{|\alpha|}\tilde{u}}{\partial x_1^{\alpha_1} \dots \partial x_n^{\alpha_n}}$  and

$$m_{\alpha,p} = \int_{\mathbb{R}^n} p(z)z^\alpha dz.$$

Neglecting in (8) the terms involving partial derivatives with order greater than two we obtain

$$s\tilde{u}(x, s) - u_0(x) = -\tilde{M}(s)\left(v \cdot \nabla \tilde{u}(x, s) - \nabla \cdot (D \nabla \tilde{u})(x, s)\right), \quad (9)$$

where  $v$  is the vector with components  $v_i = \frac{1}{t_1} \int_{\mathbb{R}^n} p(z)z_i dz$ , and  $D$  is the matrix of order  $n$  defined by  $D_{ii} = \frac{1}{2t_1} \int_{\mathbb{R}^n} p(z)z_i^2 dz$  and  $D_{ij} = \frac{1}{t_1} \int_{\mathbb{R}^n} p(z)z_i z_j dz$ ,  $i \neq j$ . We remark that equation (9) can be also obtained with convenient modifications if the pdf  $\phi$  has a compact support in  $\mathbb{R}^n$ .

We observe that the one dimension version of the equation (9) was used for instance in [5], [6], [8] and [15] to simulate tracer transport in porous media when  $p$  is a Gaussian pdf and  $\phi$  is the truncated power law pdf

$$\phi(t) = \frac{(1+t/t_1)^{-1-\beta}}{t_1 r^\beta \Gamma(-\beta, r)} \exp\left(-\frac{t_1+t}{t_2}\right), \quad r = \frac{t_1}{t_2}, t_1 < t_2, \quad 0 \leq \beta \leq 2,$$

where  $\Gamma$  is the incomplete Gamma function. In these papers, the integral terms of equation (6) were replaced by summations over  $z$ .

Another alternative that can be considered to avoid the pathological behavior of the classical diffusion equation (4) consist in the introduction of an hyperbolic or non-Fickian correction as been proposed, e.g., in [17], [21]. One possible approach is to assume that the dispersive mass flux  $J_{dis}$  satisfies the following differential equation

$$\tau \frac{\partial J_{dis}}{\partial t}(x, t) + J_{dis}(x, t) = -D_d \nabla u(x, t), \quad (10)$$

where  $\tau$  is a delay parameter. Note that the left hand side of (10) is a first order approximation of the left hand side of  $J_{dis}(x, t + \tau) = -D_d \nabla u(x, t)$ , which means that the dispersion mass flux at the point  $x$  and time  $t + \tau$  depends on the gradient of the concentration at the same point but at a delayed time. Equation (10) leads to

$$J_{dis}(t) = - \int_0^t K_{er}(t - s) D_d \nabla u(s) ds, \quad (11)$$

provided that  $J_{dis}(0) = 0$ . In (11)  $K_{er}$  is given by  $K_{er}(t) = \frac{1}{\tau} e^{-\frac{t}{\tau}}$ . Combining the partition (2), where  $J_{dif}$  and  $J_{dis}$  are given by (3) and (11), respectively, with (1) we obtain the integro-differential equation

$$\frac{\partial u}{\partial t} + \nabla \cdot (uv) - \nabla \cdot (D_m \nabla u) = \int_0^t K_{er}(t - s) \nabla \cdot (D_d \nabla u)(s) ds \quad (12)$$

which replaces (5). The mathematical and numerical analysis of initial boundary value problems based on integro-differential equations of type (12) were studied for instance in [1], [3], [10], [11], [13], [14] and [25].

The objective of this paper is to illustrate the capacity of the three different classes of models introduced to simulate the experiments presented in [2] and [29]. These experiments are characterized by a non-Fickian behavior, i.e., deviation from the classical diffusion equation (5) which can be consequence of the existence of preferential flow paths that strongly influence both water and tracer transport ([22]). In Section 2 we describe the numerical procedures used in the numerical simulations presented in Section 3. In this last section such numerical simulations are compared with experimental results. In Section 4 we summarize some conclusions. We point out that to the best of our knowledge, this is the first work where the validation of mathematical models based on integro-differential equations of type (12) is considered.

## 2 BTCs

In this section, we test and validate the models by fitting breakthrough curves (BTCs) resulting from laboratory tracer tests. These curves describe the evolution of the tracer

concentration at specific point of the spatial domain where the tracer transport occurs. Experimentally BTCs show early arrival times and long later time tails (see for instance [2], [18] and [29]).

A common assumption in the validation of mathematical models in the context of tracer transport is to consider that the experiments can be described by a one dimension model, that is, if the diffusion process occurs in a cylinder, then the behavior of the tracer in a perpendicular disc to the axis of the cylinder is well described by its behavior at the center of such disc. Therefore, equations (5), (9) and (12) are defined in the domain  $(0, T] \times (0, L)$  and they are completed with the initial condition  $u(x, t) = u_0(x), x \in (0, L)$ , and boundary conditions of the following type

$$u(0, t) = u_I(t), u(L, t) = 0, t \in (0, T],$$

where the first condition defines the injected fluid while the last one means that all the fluid that attains the end of the spatial domain is removed. In  $[0, T] \times [0, L]$  we introduce a grid  $\{(x_i, t_n), i = 0, \dots, N_x, n = 0, \dots, N_t\}$ , where  $x_0 = 0, x_{N_x} = L, x_i - x_{i-1} = h, t_0 = 0, t_{N_t} = T$  and  $t_n - t_{n-1} = \Delta t$ .

The numerical curves are obtained fitting the BTCs curves using the the root mean square error (RMSE) defined by

$$RMSE = \left( \frac{1}{N_t} \sum_{n=1}^{N_t} (u^n - u_h^n)^2 \right)^{1/2},$$

where  $N_t$  is the number of measurements at the prescribed point and  $u_h^n$  is the corresponding approximation defined by a discretization of the classical diffusion equation (5) or (9) or (12).

We remark that equation (12) for a particular choice of  $\phi(t)$  leads to equation (5). In fact if  $\phi(t) = \lambda e^{-\lambda t}$  and  $t_1 = \lambda^{-1}$  then  $\tilde{\phi}(s) = \frac{1}{1 + \lambda^{-1}s}$  and  $\tilde{M}(s) = 1$ . While the best-fit BTCs based on (5) and (12) are computed using the publicly available CTRW toolbox ([7]), the best-fit BTCs based on (12) are computed using a numerical scheme previous studied by the authors in [1], [13] and [14] which, for one dimension, can be written in the following form

$$D_{-t}u_h^{n+1} + vD_c(u_h^{n+1}) - D_mD_2u_h^{n+1} = D_d\Delta t \sum_{\ell=1}^n K_{er}(t_{n+1} - t_\ell)D_2u_h^\ell, \quad (13)$$

where  $D_{-t}$  denotes the usual backward finite difference operator in time,  $D_c$  and  $D_2$  represent the second order centered finite difference operators which approximate the first and the second spatial derivatives, respectively. In this case the minimization of the RMSE is carried out using built-in routines of Matlab (version 7.9.0 (R2009b)). To avoid possible influence on the numerical solution, the outlet boundary condition is imposed far enough from the grid point used for the computation of the BTCs.

### 3 Validation

#### 3.1 Data set 1

In an already classical experiment, Scheidegger [29] used homogeneous Berea sandstone core columns to investigate the accuracy of the classical diffusion model in simulating tracer transport in porous media. During the experiment, columns of different lengths were first fully saturated with tracer and subsequently flushed with clean liquid. The resulting tracer BTCs at the outflow boundary were measured and compared with the ones predicted by the classical diffusion model.

We test the introduced models using typical data from one of these experiments. In this case, the column was  $7.62 \times 10^{-1}$  meters (m) long and  $5.08 \times 10^{-2}$  m in diameter, the clean liquid was injected at a rate equal to 1.73 cubic centimeters per minute ( $\text{cm}^3/\text{min}$ ), and the porosity of the core was 0.204. This gives an average velocity of  $4.18 \times 10^{-3}$  m/min. We consider  $u_I = 1$ , for  $t \in (0, T]$ . In Figure 1 (a) we show the experimental data and the best-fit curves obtained with the models (5) and (12), and the best-fit curves for models (12) and (9) are shown in Figure 1 (b).

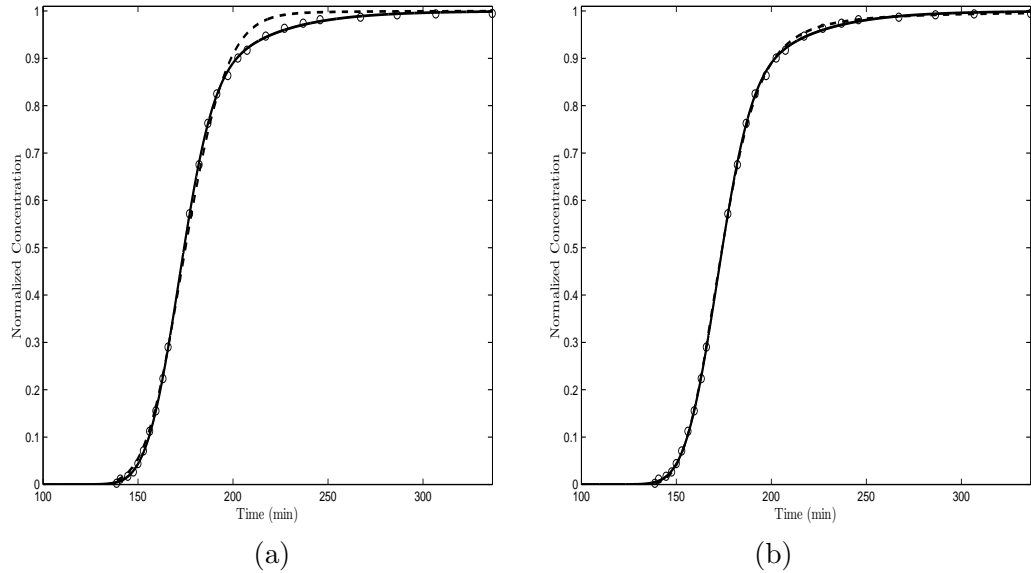


Figure 1: Experimental data set 1 and the best-fit BTCs: (a) - models (5) (dash line) and (12)(solid line); (b)-models (12) (solid line) and (9) (dash line).

A quick observation of Figure 1 (a) indicates that the model (12) captures the transport dynamics quite well. However, the model (5) fails to describe the data, especially at later times, since it can not reproduce the long tail, a typical indication of non-Fickian transport.

This result for the classical diffusion model (5) is in line with the findings of Scheidegger. The values of the two models constants and the RMSE are listed in Table 1. As indicated by the given results, the application of the proposed model leads to a reduction of about 79% in the RMSE.

Now we compare the results obtained for the integro-differential model (12) with the results for the CTRW model (9). As shown in Figure 1 (b), there is only a small discrepancy between them. The RMSE values,  $3.66 \times 10^{-3}$  and  $5.11 \times 10^{-3}$ , respectively, suggest that the integro-differential model fits the data slightly better. Here and in the following, we omitted the values of  $t_1$  and  $t_2$  in the model (9). They are consistently very small, and very large, respectively, when compared to the time scale.

Parameters	model (5)	model (9)	model (12)
$v$ (m/min)	$4.65 \times 10^{-3}$	$7.23 \times 10^{-3}$	$4.27 \times 10^{-3}$
$D$ (m <sup>2</sup> /min)	$1.35 \times 10^{-5}$	$7.86 \times 10^{-6}$	
$D_m$ (m <sup>2</sup> /min)			$1.08 \times 10^{-5}$
$D_d$ (m <sup>2</sup> /min)			$1.76 \times 10^{-5}$
$\tau$ (min)			25.52
$\beta$		1.58	
RMSE	$1.72 \times 10^{-2}$	$5.11 \times 10^{-3}$	$3.66 \times 10^{-3}$

Table 1: Fitting parameters for the results of Figure 1 and RMSE values.

### 3.2 Data set 2

The second group of data is the result of tracer displacement experiments through homogeneous sand columns reported in [2]. Next, we briefly describe the setup and we refer to that paper for all other experimental details. The columns were incrementally packed with sand particles of different sizes. The diameter of most of the sand particles lie in the range of 0.1 – 0.71 millimeters. We consider the results for two columns: Column 1, 11 cm in diameter and 10 cm long; and Column 2, also 11 cm in diameter but 40 cm long. The transport experiment was conducted under initially unsaturated conditions, with the water content of 0.24 for Column 1 and of 0.18 for Column 2. A pulse tracer at the flow rate of  $4.20 \times 10^{-2}$  cm/min was applied at the top of both columns within the time period of 140 seconds (s) for the smaller column and of 107 s for the longer one. The respective average velocities were  $1.86 \times 10^{-1}$  cm/min and  $2.28 \times 10^{-1}$  cm/min. After the pulse, water was injected at the same rate. To simulate this scenario, for Column 1 we set at the inlet boundary  $u_I = 4.16 \times 10^{-2}$  for  $t \leq t_I = 2.33$  min and  $u_I = 0$  for  $t > t_I$ , and for Column 2 the inlet boundary is defined by  $u_I = 5.77 \times 10^{-2}$  for  $t \leq t_I = 1.78$  min and  $u_I = 0$  for  $t > t_I$ . The observed and fitted BTCs for the models are plotted in Figure 2 for Column 1 and in Figure 3 for Column 2.

In particular, Figures 2 and 3 show that the agreement for the classical diffusion model

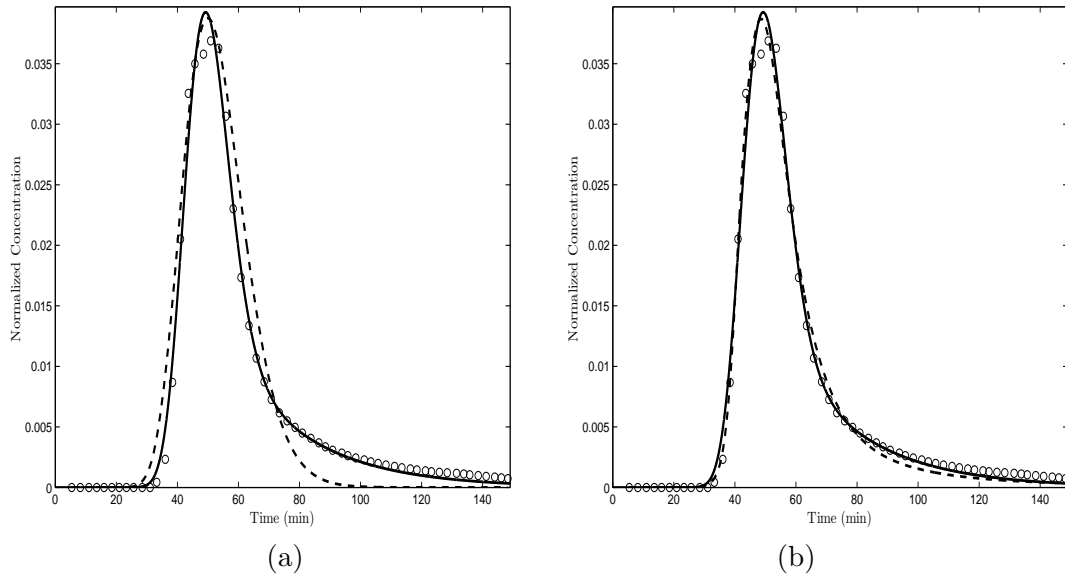


Figure 2: Experimental data set 2 and the best-fit BTCs for Column 1: (a) - model (5)(dash line) and model (12) (solid line); (b)- model (9) (dash line) and model (12) (solid line) .

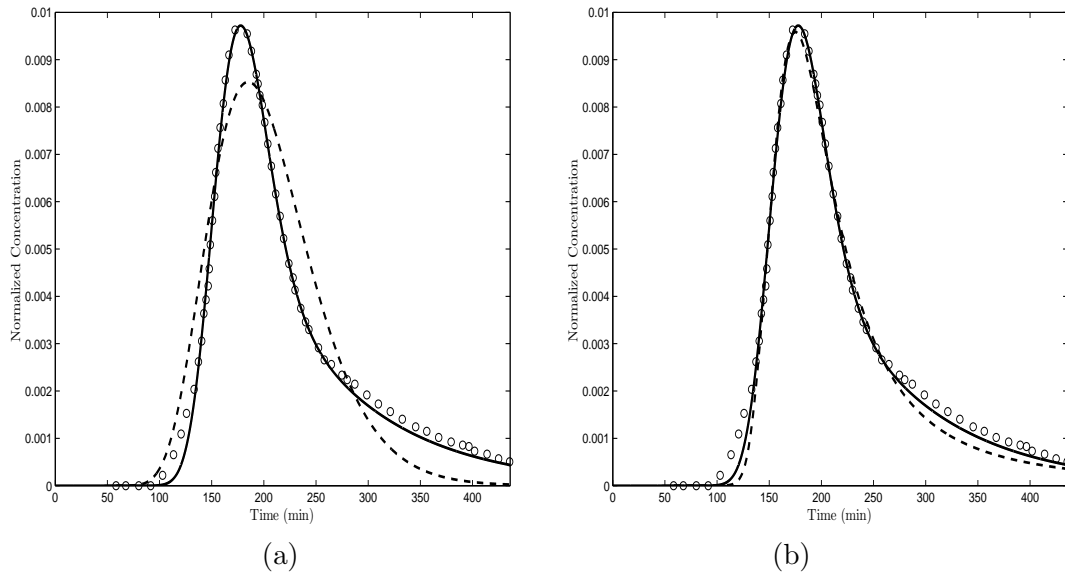


Figure 3: Experimental data set 2 and the best-fit BTCs for Column 2: (a) - model (5)(dash line) and model (12) (solid line); (b)- model (9) (dash line) and model (12) (solid line) .

is very poor. This is especially true at later times, where the BTC possesses a heavy tail. On the other hand, the integro-differential model (12) captures the BTC behavior much better. The RMSEs presented in Tables 2 and 3 confirm this conclusion.

Parameters	model (5)	model (9)	model (12)
$v$ (m/min)	$1.88 \times 10^{-1}$	1.10	$1.69 \times 10^{-1}$
$D$ (m <sup>2</sup> /min)	$3.69 \times 10^{-2}$	$2.92 \times 10^{-2}$	
$D_m$ (m <sup>2</sup> /min)			$2.59 \times 10^{-1}$
$D_d$ (m <sup>2</sup> /min)			$10^{-1}$
$\tau$ (min)			15.95
$\beta$		1.1	
RMSE	$2.5 \times 10^{-3}$	$9.77 \times 10^{-4}$	$9.53 \times 10^{-4}$

Table 2: Fitting parameters for the models plotted in Figure 2 and RMSE values.

Parameters	model (5)	model (9)	model (12)
$v$ (m/min)	$1.90 \times 10^{-1}$	2.88	$1.74 \times 10^{-1}$
$D$ (m <sup>2</sup> /min)	$2.37 \times 10^{-1}$	$1.88 \times 10^{-1}$	
$D_m$ (m <sup>2</sup> /min)			$1.16 \times 10^{-1}$
$D_d$ (m <sup>2</sup> /min)			$4.25 \times 10^{-1}$
$\tau$ (min)			42.14
$\beta$		0.97	
RMSE	$9.64 \times 10^{-4}$	$3.43 \times 10^{-4}$	$1.91 \times 10^{-4}$

Table 3: Fitting parameters for the models plotted in Figure 3 and RMSE values.

## 4 Conclusions

In this paper three different classes of diffusion models are compared considering tracer transport experimental data: the classical diffusion model (5), the CTRW model (9) and the integro-differential model (12). The classical diffusion model is established assuming Fick's law for the mass flux while the CTRW model is established considering that the particles perform jumps and between consecutive jumps the particles wait for a random time. The randomness of the transport is described by a joint pdf for the waiting time and for the length of the jump. The integro-differential model is constructed by modifying Fick's law considering that the mass flux at a certain time depends on the gradient of the concentration at a delayed time.

The numerical simulations show that the classical diffusion model does not capture the long tails of the BTCs at later times while the CTRW model and the integro-differential model are able to reproduce this non-Fickian behavior leading the last model to a greater reduction of RMSE.

## Acknowledgements

This work was partially supported by the Centro de Matematica da Universidade de Coimbra (CMUC), funded by the European Regional Development Fund through the program COMPETE and by the Portuguese Government through the FCT under the project PEst-C/MAT/UI0324/2013 and project UTAustin/MAT/0066/2008.

## References

- [1] S. BARBEIRO, J.A. FERREIRA, L. PINTO,  *$H^1$ - second order convergent estimates for non Fickian models*, Appl. Numer. Math. **61** (2011) 201–215.
- [2] M. BROMLY, C. HINZ, *Non-Fickian transport in homogeneous unsaturated repacked sand*, Water Resour. Res. **40** (2004) W07402.
- [3] J. CANNON, Y. LIU, *A priori  $L^2$  error estimates for finite element methods for nonlinear diffusion equations with memory*, SIAM J. Numer. Anal. **27** (1990) 595–607.
- [4] H-T. CHEN AND K-C. LIU *Analysis of non-Fickian diffusion problems in a composite medium*, Comput. Phys. Commun. **10** (2003) 31–42.
- [5] A. CORTIS, B. BERKOWITZ, *Anomalous transport in classical soil and sand columns*, Soil. Sci. Soc. Am. J. **68** (2004) 139–148.
- [6] A. CORTIS, Y. CHEN, H. SCHER, B. BERKOWITZ, *Quantitative characterization of pore-scale disorder effects on transport in homogeneous granular media*, Phys. Rev. E **70** (2004) 041108.
- [7] A. CORTIS, B. BERKOWITZ, *Computing anomalous contaminant transport in porous media: the CTRW MATLAB toolbox*, Groundwater **43** (2005) 947–950.
- [8] M. DENTZ, A. CORTIS, H. SCHER, B. BERKOWITZ, *Time behavior of solute transport in heterogeneous media: transition from anomalous to normal transport*, Adv. Water Resour. **27** (2004) 15–173.
- [9] J. DOUGLAS JR, *Superconvergence in the pressure in the simulation of miscible displacement*, SIAM J. Numer. Anal. **22** (1985) 962–969.
- [10] R. EWING, R. LAZAROV, Y. LIN, *Finite volume element approximations of nonlocal in time one-dimensional flows in porous media*, Computing **64** (2000) 17–182.
- [11] R. EWING, Y. LIN, T. SUN, J. WANG, S. ZHANG, *Sharp  $L^2$  error estimates and superconvergence of mixed finite element methods for non-Fickian flows in porous media*, SIAM J. Numer. Anal. **40** (2002) 138–160.

- [12] R. E. EWING AND M. F. WHEELER, *Galerkin methods for miscible displacement problems in porous media*, SIAM J. Numer. Anal. **17** (1980) 351–365.
- [13] J.A. FERREIRA, E. GUDINO, P. DE OLIVEIRA, *A second order approximation for quasilinear Non-Fickian models*, Comput. Meth. Appl. Math. **13** (2013) 471–493.
- [14] J.A. FERREIRA, L. PINTO, G. ROMANAZZI, *Supraconvergence and supercloseness in Volterra equations*, Appl. Numer. Math. **62** (2012) 1718–1739.
- [15] G. GAOA, H. ZHANG, S. FENGA, G. HUANG, X. MAO, *Comparison of alternative models for simulating anomalous solute transport in a large heterogeneous soil column*, J. Hydrol. **377** (2009) 391–404.
- [16] L.W. GELHAR, C. WELTY, K. R. REHFELDT, *A critical review of data on field-scale dispersion in aquifers*, Water Resour. Res. **28** (1992) 1955–1974.
- [17] S.M. HASSAHIZADEH, *On the transient non-Fickian dispersion theory*, Transp. Porous Media **23** (1996) 107–124.
- [18] K. HUANG, N. TORIDE, M. VAN GENUCHTEN, *Experimental investigation of solute transport in large, homogeneous, and heterogeneous, saturated soil columns*, Transp. Porous Media **18** (1995) 283–302.
- [19] M. LEVY, B. BERKOWITZ, *Measurement and analysis of non-Fickian dispersion in heterogeneous porous media*, J. Contam. Hydrol. **64** (2003) 203–226.
- [20] D.M. MACKAY D.L. FREYBERG, P.B. ROBERTS , J.A. CHERRY, *A natural gradient experiment on solute transport in a sand aquifer: 1. Approach and overview of plume movement*, Water Resour. Res. **22** (1986) 2017–29.
- [21] S. P. NEUMAN, D. M. TARTAKOVSKI, *Perspectives on theories of non-Fickian transport in heterogeneous media*, Adv. Water Resour. **32** (2008) 670–680.
- [22] S. OSWALD, W. KINZELBACHA, A. GREINERB, G. BRIXC, *Observation of flow and transport processes in artificial porous media via magnetic resonance imaging in three dimensions*, Geoderma **80** (1997) 417–429.
- [23] D. W. PEACEMAN, *Improved treatment of dispersion in numerical calculation of multidimensional miscible displacement*, Soc. Petrol. Eng. **6** (1966) 213–216.
- [24] T. F. RUSSEL AND M. F; WHEELER, *Finite element and finite difference methods for continuous flows in porous media*, in *The Mathematics of Reservoir Simulation*, SIAM, Philadelphia, 1983, 35–106.
- [25] R. SINHA, R. EWING, R. LAZAROV, *Some new error estimates of a semidiscrete finite volume element method for a parabolic integro-differential equation with nonsmooth initial data*, SIAM J. Numer. Anal. **43** (2006) 2320–2344.

- [26] C.R. SIDLE, B. NILSSON, M. HANSEN, J. FREDERICIA, *Spatially varying hydraulic and solute transport characteristics of a fractured till determined by field tracer tests, Funen, Denmark*, Water Resour. Res. **34** (1998) 251–2527.
- [27] S. E. SILLIMAN, L.F. KONIKOW, C. I. VOSS, *Laboratory investigation of longitudinal dispersion in anisotropic porous media*, Water Resour. Res. **11** (1987) 2145–211.
- [28] A. SETTARI, H. S. PRICE AND T. DUPONT, *Development and application of variational methods for simulation of miscible displacement in porous media*, Soc. Petrol. Eng. **17** (1977) 228–246.
- [29] A. SCHEIDEGGER, *An evaluation of the accuracy of the diffusivity equation for describing miscible displacement in porous media*, in *Proceedings of the Theory of Fluid Flow in Porous Media Conferenc*, University of Oklahoma, 1959, 101–116.
- [30] S.P. STERNBERG, J. H. CUSHMAN, R.A. GREENKORN, *Laboratory observation of nonlocal dispersion*, Transp. Porous Media **23** (1996) 135–11.